Improving the Force Model of SGP4 using Neural Network

Hans Carrillo*[1], Edna Segura†[1], Rosario López‡[1], and Juan Félix San-Juan§[1]

[1]Scientific Computing & Technological Innovation (SCoTIC), University of La Rioja, Logroño, La Rioja, Spain.

Abstract

The trajectory of any resident space object (RSO) can be determined using three different orbit propagation methods. Special Perturbation (SP) propagators use numerical techniques to integrate the equations of motion, including a complete and accurate force model. SP propagators provide very accurate orbit predictions, but the high computational cost limits the performance of this approach. General Perturbation (GP) propagators apply perturbation theories to develop an approximate analytical solution to the equations of motion. GP propagators consider simplified force models, which limit their accuracy. However, these propagators perform much faster than numerical methods. Finally, the third type is the semi-analytical propagators, which combine the strengths of SP and GP propagators. In either case, an orbit propagation program depends uniquely on the initial states and some physical parameters to make its predictions.

The hybrid methodology was introduced in 2008. It is a non-invasive technique that improves the accuracy of any orbit propagator without increasing the computational cost. This methodology has been applied to different SP, GP and semianalitical propagators. In [1, 2] different families of hybrid orbit propagators based on statistical time series techniques were developed, whereas in [3, 4, 5] the proposed propagators were based on machine learning techniques.

In this work, we apply the hybrid methodology to improve the force model and the integration method of the well-known SGP4 orbit propagator [6, 7] using neural network (NN). The new propagator is named HSGP4. The NN is trained using the difference in the argument of latitude between accuracy ephemeris and SGP4 for Galileo-type orbits.

For this experiment, we consider 180 of the 312 time series used in [5]. This reduced set only includes time series with positive trends in the first revolutions, of which approximately 60%, 110 series, are used during the training and validation processes of the forecasting model. In contrast, approximately 40%, 70 series, are reserved for evaluating the generalization capability of the model. On the other hand, each of the 110 series is divided into two subseries: 14 revolutions, which represent approximately 200 hours, constitute the training interval used for fitting the model's parameters and the following 6 revolutions are used for validation. It is worth noting that the first two revolutions are necessary to start the network predictions.

The NN architecture [8, 5] consists of an input layer of 169 neurons, two hidden layers with 256 and 128 neurons, and an output layer with one neuron. The first hidden layer applies a linear function as activation function, whereas the exponential linear unit (elu) for the second. The batch size parameter is 64, and the optimizer to determine weights and bias of the connection among the nodes was given by *adam* (adaptive moment estimation). The cost function to use in this work will be the popular error score RMSE (root mean square error).

Fig. 1 shows the box-and-whisker plots of the distance errors between AIDA and SGP4 for the 110 TLEs of the predictive model. The time span considered is up to 12 days from the epoch of the TLE. The relatively small values of the median in this Figure is a consequence that more of the 50% of the time series ε^θ have small values of the trend components.

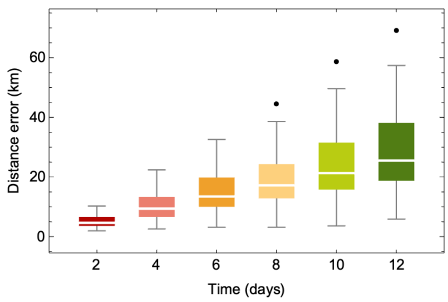

Figure 1: Box-and-whisker plots showing the distance error (km) between AIDA and SGP4 for the sample of 110 TLEs and a time span of 12 days.

Fig. 2 shows the box-and-whisker plots of the distance errors between AIDA and BestHSGP4 for the dataset of 110 TLEs. The BestHSGP4 propagator is obtained when the time series of the error is zero, $\varepsilon^\theta = 0$, that is, $\theta^{\rm AIDA} = \theta^{\rm SGP4}$. Compared with the

*Email: hans-mauricio.carrillo@unirioja.es.
†Email: edna-viviana.segura@alum.unirioja.es.
‡Email: rosario.lopez@unirioja.es.
§Email: juanfelix.sanjuan@unirioja.es.

previous box plot, whereas the maximum distance of SGP4 is approximately 68.94 km after twelve days, the maximum error of BestHSGP4 is reduced to only 1.96 km.

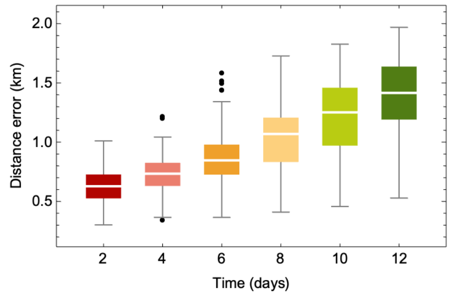

Figure 2: Box-and-whisker plots showing the distance error (km) between AIDA and BestHSGP4 for the sample of 110 TLEs and a time span of 12 days.

Fig. 3 shows the box-and-whisker plots of the distance error between AIDA and SGP4 for the unseen 70 TLEs used for testing the predictive model. The time span considered in this process is also 12 days. In this sample, the maximum distance error of SGP4 is approximately 23.88 km after twelve days, this is about 45 km less than the dataset used to create the predictive model. The outliers from the eight day are due to the dispersion of the time series ε^{θ}.

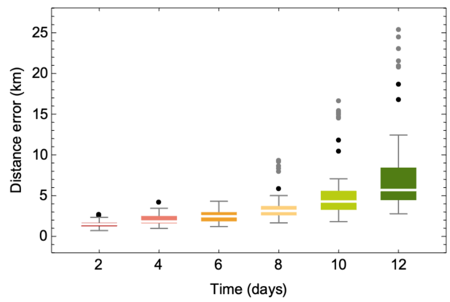

Figure 3: Box-and-whisker plots showing the distance error (km) between AIDA and SGP4 for the sample of 70 TLEs and a time span of 12 days.

Fig. 4 shows the box-and-whisker plots of the distance errors between AIDA and BestHSGP4 for the same 70 TLEs set. The Fig. 2 indicates that the the magnitude of the BestHSGP4 distance error obtained with the 70 TLEs set is similar to the 110 TLE set.

Once the NN model has been trained and included in the hybrid propagation module (HSGP4), we evaluate the performance of the new propagator. First, the HSGP4 is compared with SGP4 so as to assess how well the model fits at 2, 4, 6, 8, 10, and 12 days of propagation for the known 110 TLEs used when the model was fit. Fig. 5 depicts the box-and-whisker plots of the distance errors between AIDA and HSG4.

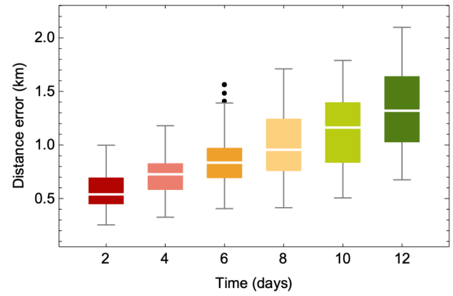

Figure 4: Box-and-whisker plots showing the distance error (km) between AIDA and BestHSGP4 for the sample of 70 TLEs and a time span of 12 days.

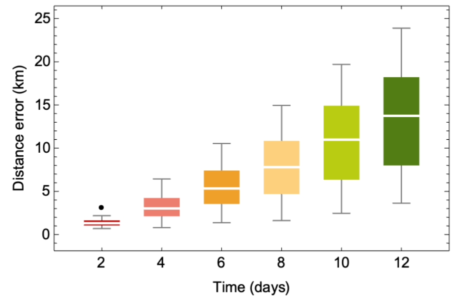

Figure 5: Box-and-whisker plots showing the distance error (km) between AIDA and HSGP4 for the sample of 110 TLEs and a time span of 12 days.

The capacity of generalization on the HSGP4 is evaluated on the remaining unseen 70 time series set. Fig. 6 depicts the box-and-whisker plots of the distance error between AIDA and HSG4.

The Q_3 value of the BestHSGP4 is small during the twelve propagation days and their values similar to the obtained with the 110 TLE set. However, the value of HSGP4 grows as quickly as the previous 110 but remains slight below the SGP4 value, less than 1 km. It is due to the values of the trend of the 70 TLE set is less than the 110 set.

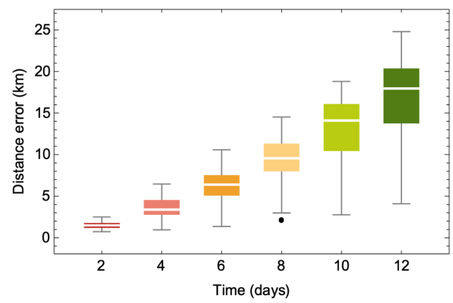

Figure 6: Box-and-whisker plots showing the distance error (km) between AIDA and HSGP4 for the sample of 70 TLEs and a time span of 12 days.

The two TLE datasets used for training and testing the HSGP4 propagator follow the same behaviour, as can be seen in Fig. 5 and 6.

Fig. 7 and 8 show two of the best predictions of the argument of latitude of the 70 time series set. The forecasting model only needs the first two revolutions to inicializate the calculus process. In both cases, the model initially reproduces the periodic behaviour of the series. However, as time progresses, the neural network model loses its capability to recognize this periodic pattern while maintaining the trend.

Table 1 and 2 show the distance error between HSGP4 and AIDA for the TLEs 9 and 23. As can be seen, the distance error of HSGP4, in both TLEs, is close to the obtained with BestHSGP4 and reduced by approximately 45 km respect to SGP4

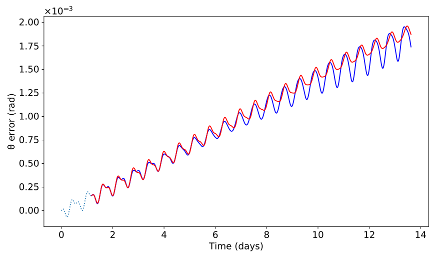

Figure 7: Red represents the predictions of the argument of latitude using the HSGP4 propagator, while in blue the precise data for the test TLE 9.

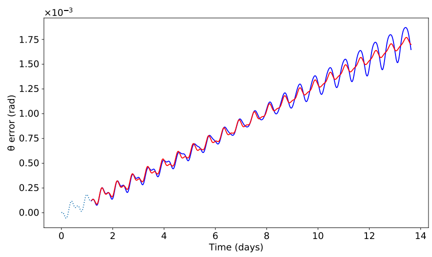

Figure 8: Red represents the predictions of the argument of latitude using the HSGP4 propagator, while in blue the precise data for the test TLE 23.

Table 1: Maximum distance errors in km between HSGP4 and AIDA for the TLE 9 after 2, 4, 6, 8, 10, and 12 propagation days

Error	**2**	**4**	**6**	**8**	**10**	**12**
SGP4	8.36	18.03	25.82	35.07	44.71	52.41
BestHSGP4	0.88	0.94	1.07	1.46	1.74	2.09
HSGP4	0.91	1.15	1.89	3.65	4.90	5.52

Table 2: Maximum distance errors in km between HSGP4 and AIDA for the TLE 23 after 2, 4, 6, 8, 10, and 12 propagation days

Error	**2**	**4**	**6**	**8**	**10**	**12**
SGP4	7.59	15.79	23.25	31.32	41.37	49.12
BestHSGP4	0.80	0.82	0.85	0.92	1.29	1.65
HSGP4	1.07	1.38	1.38	1.99	2.77	4.09

Acknowlegdgements

HC acknowledge to the FPI grant from the University and the Comunidad Autónoma de La Rioja 2019.

References

[1] J. F. San-Juan, M. San-Martín, I. Pérez, and R. López, "Hybrid perturbation methods based on statistical time series models," *Advances in Space Research*, vol. 57, no. 8, pp. 1641–1651, April 2016, Advances in Asteroid and Space Debris Science and Technology - Part 2.

[2] M. San-Martín, I. Pérez, and J. F. San-Juan, "Hybrid methods around the critical inclination," *Advances in the Astronautical Sciences*, vol. 156, pp. 679–693, 2016, paper AAS 15-540.

[3] J. F. San-Juan, I. Pérez, M. San-Martín, and E. P. Vergara, "Hybrid SGP4 orbit propagator," *Acta Astronautica*, vol. 137, pp. 254–260, August 2017.

[4] J. F. San-Juan, M. San-Martín, and I. Pérez, "Application of the hybrid methodology to SGP4," *Advances in the Astronautical Sciences*, vol. 158, pp. 685–696, 2016, paper AAS 16-311.

[5] E. Segura, H. Carrillo, R. López, M. Pérez, I. San-Martín, and J. F. San-Juan, "Deep learning hsgp4: Hyperparameters analysis," in *Proceedings 31st AAS/AIAA Space Flight Mechanics Meeting.* Charlotte, NC, USA: American Institute of Aeronautics and Astronautics, Feb 1-4 2021, paper AAS 21-241.

[6] F. R. Hoots and R. L. Roehrich, "Models for propagation of the NORAD element sets," U.S. Air Force Aerospace Defense Command, Colorado Springs, CO, USA, Spacetrack Report #3, 1980.

[7] D. A. Vallado, P. Crawford, R. Hujsak, and T. S. Kelso, "Revisiting spacetrack report #3," in *Proceedings 2006 AIAA/AAS Astrodynamics Specialist Conference and Exhibit*, vol. 3. Keystone, CO, USA: American Institute of Aeronautics and Astronautics, August 2006, pp. 1984–2071, paper AIAA 2006-6753.

[8] H. Carrillo, E. Segura, R. López, I. Pérez, and J. F. San-Juan, "Hybrid orbit propagator based on neural networks. multivariate time series forecasting approach," in *16th International Conference on Soft Computing Models in Industrial and Environmental Applications (SOCO 2021)*, H. Sanjurjo González, I. Pastor López, P. García Bringas, H. Quintián, and E. Corchado, Eds. Cham: Springer International Publishing, 2022, pp. 695–705.